doi:10.6041/j.issn.1000-1298.2016.06.027

# Experiment on Biomass Rotary Gasifier with Bed Material

Yu Chunjiang Zhai Xianghe Xie Guilin Zhou Yusheng Tu Hanchao
(*State Key Laboratory of Clean Energy Utilization*, *Zhejiang University*, *Hangzhou* 310027, *China*)

**Abstract**: In order to combine the traditional rotary mechanical disturbance characteristic with the inert bed material heat storage properties, a new type of rotary gasifier was designed. On the basis of the new type of rotary gasifier, a staged gasification and combustion experimental platform was designed and the thermal state test of the system was completed. The effects of rotational speed, equivalence ratio, temperature and other parameters on the gasification reaction system were investigated. The experimental results showed that when rotary furnace speed was controlled at 1 ~ 4 r/min, the rotary furnace mixed disturbance characteristics were enhanced with the increase of rotary speed, and temperature distribution was more uniform in the furnace, different parameters were improved in the experimental range, good gas production was got at rotary furnace speed of 3 r/min. When temperature was controlled in the range of 550 ~ 700℃, the gasification parameters were increased with the increase of temperature, and gas calorific value and gasification efficiency were affected greatly by temperature. Under the experimental conditions with temperature of 600 ~ 650℃, the calorific value of combustible gas, gasification efficiency and other indicators were greatly improved. The equivalent ratio (ER) was changed in the range of 0.2 ~ 0.4, and it had great impact on gas production of the indicators, with the increase of equivalence ratio, the gas production rate and bed temperature were increased to a certain degree, the change trend of other gasification parameters were firstly increased and then decreased, good gasification results were obtained with ER of 0.3. The typical result showed that gas composition of rotary gasifier was close to that of the fluidized bed, considering the sensible enthalpy, the gasification efficiency was about 79.3% and the carbon conversion rate was about 81.3%. The gasifier energy balance was calculated, and the output efficiency of the system was 86.8%, with heat dissipation as main energy loss way. It was found from the separation of the bottom ash with bed material that about 86% of the total ash content was remained in the bed material area, and more than 90% of it was distributed in the bottom of the bed material area. Experimental results were optimized by controlling the variables for operation and design of new type of gasifier improvement to provide reference.

**Key words**: rotary type gasifier; bed material; biomass; gasification efficiency

## 0 Introduction

Traditional rotary reactor is mainly used in powder or mineral materials primary processing industries[1]. The furnace mechanical perturbations of rotary reactor can promote material mixing and heat transfer, since the characteristic on the material shape and size adaptable[2-3]. Nearly three decades, researchers at home and abroad for the rotary furnace launched a series of studies in the field of waste incineration, mainly for sludge, medical waste and other low calorific value solid waste pyrolysis incineration[4-11].

For traditional rotary incinerator, the reactant is the solid materials and air for combustion. Material is driven by rotational movement in the reactor and gradually moved from one end to the other end, and burnout during the contact with air. In order to increase the controllability of the furnace materials thermochemical reaction temperature and further strengthen the material gas-solid phase reaction involving heat and mass transfer process, it is a feasible way that adding inert bed material particles large heat capacity in the reaction system, after reference fluidized reaction conditions[12-13]. In this paper, the conventional rotary reactor is improved to store relatively large amounts of inert bed material, and use the rotary motion of the furnace to drive bed material particle motion, similar to fluidization of fluidization wind in the fluidized bed, to achieve internal disturbances mixed in rotary reactor. By

Received date: 2016-01-06 Accepted date: 2016-01-31
Supported by National Natural Science Foundation of China (Grant No. 51336008)
Corresponding author: Yu Chunjiang, Professor. E-mail: chunjiang@zju.edu.cn. Tel: +86-0571-87952801.

exploring the influence of new type gasifier mechanical disturbance characteristics for the reaction of the fluidized medium and material, it is feasible to be verified that the improved rotary reactor applied in gasification or combustion process with high alkali biomass feedstock which need strict temperature control.

## 1 Experiment

### 1.1 Gasifier structural features

To verify the applicability and gasification performance of the new rotary gasification reactor, this paper designed the gasification program with portion of air gasification of biomass briquette[14-16]. Considering the need of bed material accumulated in the rotary reactor, a simpler solution is to increase the inclination of the cylinder arrangement, use a lower aspect ratio and close the bottom end of cylinder, as shown in Fig. 1. In this design, the inert particulate bed material was accumulated in lower portion of the reactor. During cylinder rotary, bed material was carried by the barrel wall and was sufficiently disturbed. Air as gasification medium was sent into the bed material area from the primary air inlet at the bottom of barrel. And the fuel was fed into the bed material area from the fuel inlet which was arranged at the top of barrel. Then the fuel mixed with the hot bed material and was dried, pyrolysis and complete the partial combustion and gasification reaction through contact with the air into the bed material region. Finally, product gas was discharged out of the reactor from the exhaust port installed at gas phase space. The reactor was also provided with a conventional bearing and rotary drive devices to ensure that the reactor body can steadily rotate at a set speed.

The designed rotary gasification reactor retains the advantages of traditional rotary reactor that better mechanical disturbance property and convenient regulation, and by introducing the bed material to strengthen the material particles surrounding heat and mass transfer. For biomass, the mutual disturbance of the bed material and the raw material particles can peel off the surface ash of the particle layer, promote char particle breakage and segregation, contributed significantly to the gasification reaction process[17-19]. On the other hand, the smaller aspect ratio design and the design concept of inert bed material stably retains in the inside of reactor can enhance the efficiency of the reactor space utilization, it is easy to ensure that the reaction time of the material and increase the efficiency of gas-solid phase reaction, and have a greater advantage in the floor area of equipment and manufacturing costs.

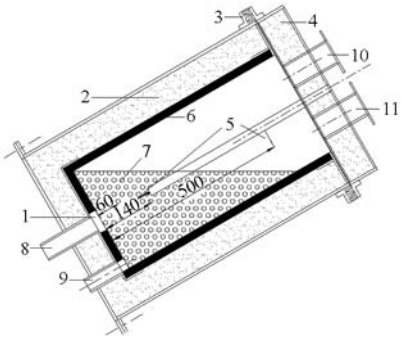


Fig. 1 Schematic diagram of new rotary gasifier

1. Porous grid plate 2. Insulation layer 3. Labyrinth seal ring 4. Fixed roof 5. Thermocouple 6. High temperature refractory 7. Bed material area 8. Primary air inlet 9. Exhaust port 10. Feed inlet 11. Product gas outlet

Compared with the traditional rotary reactor, inert bed material within the reactor has large heat capacity, which is helpful to control and maintain the temperature of the reaction zone, in the gasification combustion process, it is significant to the biomass fuel, because of the need of strict reactor temperature control and low fusion point. Besides, it is also beneficial to promote the adaptability of raw materials, and increased the equipment ability to deal with material properties fluctuations. The gasification reactor has a great potentiality of spreading and utilization in the field of high alkali biomass particles staged combustion or gasification, and can better cope with the alkali metal deposition and slagging, combustion $NO_x$ control and other issues.

### 1.2 Experimental design

In order to study the rotary biomass gasification plant performance characteristics, the author designed and built the relevant test bed. The rotary gasfication reactor shown in Fig. 1. The reactor mainly have two part: the rotary furnace which can do Rotary motion and the fixed roof, described in Fig. 1 part 4, and they are connected by an axial labyrinth seal ring.

The rotary reactor used in experiment has an aspect ratio of about 2∶1, with the angle between the horizontal and the axis of rotation about 30°, and use

the silica particles with particle size of about 3 ~ 5 mm. The gasification air is fed into the primary air inlet and then into the reactor through the porous grid plate. The porous grid plate pore size is about 1 mm, to prevent the loss of bed material leakage. The reactor outer layer is steel, while inner wall is wear resistant castable, and 80 mm insulation material disposed therebetween. So the designed reactor is adiabatic. The exhaust port located at the bottom of the reactor with an aperture plate (pore size about 1 mm) in order to discharge ash while retain the bed material in the reactor. The thermocouple protection tube is installed on the reactor fixed roof, and the built-in thermocouples are used to detect the temperature of the bottom of the bed material area, the upper space and product gas.

Fig. 2 is the stereoscopic effect diagram of the rotary gasifier, shows some detailed structures of the reactor, including seal, drive and support programs. As shown, there are four roller to support the reactor main body. A ring gear is fixed on the rotary furnace to mesh the pinion gear of reducer. The motor matched with reducer can adjust the furnace speed range from 2 to 6 r/min by frequency control. The reactor fixed roof can move axially along the fixed support shaft, which is convenient for opening and closing the roof, replacement the bed material and internal cleaning and maintenance and other operations.

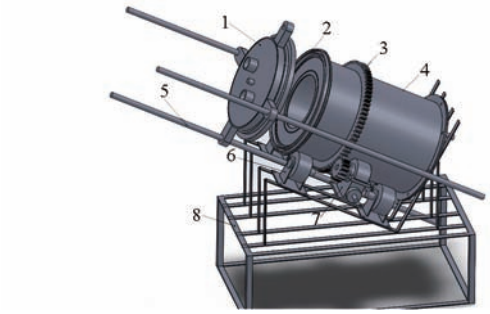


Fig. 2 Stereoscopic effect diagram of rotary gasifier

1. Fixed roof 2. Axial labyrinth seal ring 3. Ring gear 4. Reactor furnace 5. Fixed support shaft 6. Roller 7. Reducer 8. Bottom bracket

## 1.3 Thermal state experiment

### 1.3.1 Fuel characteristics

This experiment used the fuel of rod-shaped particles of cotton stalk, and raw material particles are about 4 mm in diameter, 10 mm long. The result of industrial analysis and elemental analysis shows that the largest proportion of experimental fuel is the volatile about 63%, the least proportion is ash about 7%, and C and O are the main elements of the fuel, respectively accounting for 41% and 37% of the total, with fuel heat value about 13.7 mJ/kg. All of the above indicates that cotton stalk particle fuel has the characteristics of conventional biomass fuel, with high volatile and high oxygen content. The result of ash composition analysis shows that $SiO_2$ and CaO as the main components of ash, nearly accounting for 50% ash content, meanwhile $Na_2O$ and $K_2O$ accounting for 12% ash content. The ash composition reflects the typical herbaceous agricultural biomass characteristics, high K, Na content make the thermal chemical reaction process easily to cause slagging, alkali metal deposition problem that requires more stringent control of the reaction process temperature.

### 1.3.2 Experimental system

Fig. 3 is a rotary biomass gasification reactor thermalExperimental system, which is a biomass grading combustion plant, the biomass particles partially air gasification in rotary gasification reactor to produce the product gas. Biomass particles is gasified at a low excess air ratio condition in rotary gasification reactor, and the product gas gets into the gas combustion device for combustion, completing combustion, conversion and utilization of the biomass particles. Since the temperature of the gasification process can be well controlled, the technology can be applied to combust low ash melting point straw pellet fuel. Besides, product gas can be more easily achieved with low nitrogen emissions by burning tissue, and the process route for small-scale use of biomass briquette combustion has higher application value.

The experimental system mainly includes wind system, feeding system and gasification and combustion system. The wind system has the blower, valves, rotor flow meters and preheater etc. which can provide about 300℃ gasification air as the rotary gasifier gasification medium. The feeding system can adjust the feeding amount by frequency converter to supply fuel stably. In the gasification and combustion system, the gasification process is completed in the rotary furnace, and then the product gas is passed into the combustion device to burn out. Besides, the system also includes the cyclone separator, draft fan and other auxiliary system,

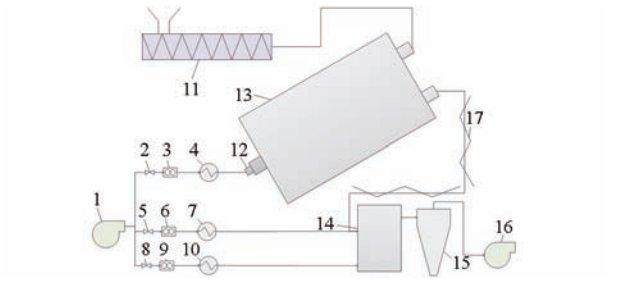


Fig. 3 Experimental system diagram of biomass rotary gasifier

1. Blower 2. Valve of gasification wind 3, 6, 9. Flowmeter 4, 7, 10. Preheater 5. Primary air valve of secondary combustion chamber 8. Secondary air valve of secondary combustion chamber 11. Feeder 12. Rotary joint 13. Rotary furnace body 14. Gas combustion device 15. Cyclone separator 16. Draft fan 17. Insulation and heating equipment

such as air preheater system, testing and sampling systems etc. During biomass gasification process, how to deal with tar is the problem that conventional gasification applications necessary to consider. Staged combustion approach used in the experiment, gas and tar can be utilized in the secondary combustion chamber under high temperature conditions. Thus, the experiment should ensure that the tar would not be condensed while getting through the line between the gasifier and secondary combustion chamber. As shown in Fig. 3, the line segment was covered with heat insulation device, which can control line temperature at above 300 ℃ to meet the conditions.

### 1.4 Experiment method

This experiment preheats the rotary furnace by directly heating the bed material, then transferring bed material at a temperature of about 400℃ into the interior of the rotary furnace, and adding ignited coal to heat up. When the temperature raised to near 550℃, adjusting the feeding amount and the amount of wind to the setting conditions. After the condition stable, starting to sample and measure, sampling each condition three times to reduce experimental error. Experimental variables need to adjust and control include the reactor rotate speed, the excess air ratio, and the internal temperature of the gasification furnace. The experiment used the control variable method to respectively study the affect of three variable to the performance of the gasifier and other parameters.

This paper use the calorific value of gas production, gas yield, gasification efficiency and carbon conversion rate, four state parameters to characterize the operating state of the reactor and evaluate the gasification effect, and the detail calculation method according to the literature [15,20].

### 1.5 Sampling and testing

During sampling process, product gas gets through coils and gas wash bottles, etc., cooled to remove the tar at a low temperature environment (−10℃). Then collecting the gas with gas collection bags and using Agilent 7890A GC to analyze the gas sample components offline, mainly to confirm the gas components of CO, $CO_2$, $H_2$, $CH_4$, $N_2$, $C_mH_n$ and others[21].

## 2 Results and discussion

### 2.1 Effect of rotary kiln speed on biomass gasification

The speed of the rotary kiln directly affects rotary furnace internal temperature distribution, disturbance degree between the material and the gasification medium, which has a great influence on the effect of gas production. In the experiment, the speed of the rotary kiln of furnace temperature distribution varying with time is shown in Fig. 4.

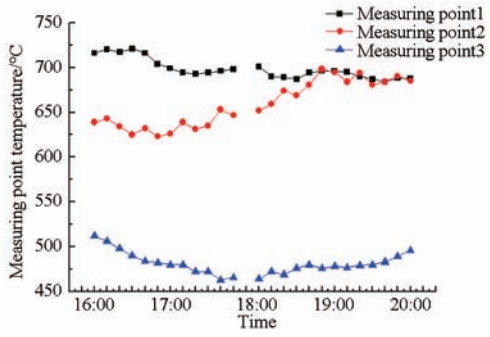


Fig. 4 Variation curve of axial temperature of rotary furnace with time

From Fig. 4, it can be seen that by 16:00 it began to enter the conditions, due to fluctuations in the feeding, rotary furnace internal temperature also changed, the two measuring points between difference was about 50℃, but bed temperature changed little overall; at the breakpoint (17:50) position rotary furnace speed increased from 2 r/min to 3 r/min, the temperature of bed materials zone appeared obvious changes, which can be seen that the measuring point 1 and 2 temperature became closer to the center, the temperature difference decreased and then became

stable. Therefor it could be inferred that the temperature in the furnace material bed zone tended to be uniform and fluctuation decreased with the speed increase, and the upper space temperature had a tendency to increase, changing characteristics of temperature revealed that the rotary furnace speed increase was favorable for material mixing and reaction process.

As seen in Fig. 5, the main gas compositions increased with the rotary speed, the overall change trend was relatively stable, especially $CO_2$, $H_2$, CO and $CH_4$. With the increase of the rotary speed, the bed material zone temperature tended to be uniform and the disturbance effect increased, which was favorable for the process of biomass pyrolysis. Meanwhile, through the biomass drying process, water was discharged into the bed material zone, with the increase of rotary speed, more water involved into the gasification reaction, $CO + H_2O \rightarrow CO_2 + H_2$, the steam reforming reaction strengthened and we got more $H_2$ and $CO_2$.

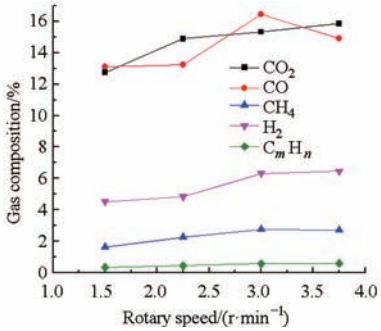


Fig. 5 Variation curves of gas composition with rotary speed

In Fig. 6, heat value and gas yield changed with the rotary speed, because the more uniform temperature and the turbulent mixing enhancement, gasification reactions in the region with the speed increased had been significantly enhanced, and we get better gas heat value and gas yield; carbon conversion and gasification efficiency changed with the rotary speed had similar trends as shown in Fig. 7.

Comprehensive analysis, the speed of the rotary kiln has an important influence on improvement of rotary furnace mixed disturbance characteristics, the furnace temperature distribution, and the characteristic parameters of biomass gasification reaction. And in a certain range with the increase of rotary speed, the heat value of the combustible gas, gas yield, gasification efficiency and carbon conversion rate were

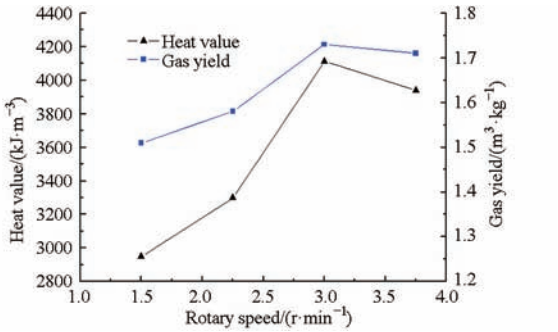


Fig. 6 Variation curves of gas LHV and gas yield with rotary speed

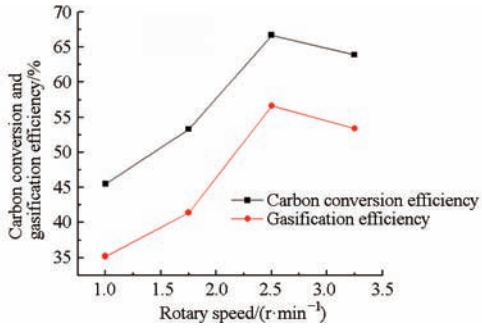


Fig. 7 Variations of carbon conversion efficiency and gasification efficiency with rotary speed

all increased. In the experiment, when the speed of the rotary kiln was in the 3 r/min, we got better gas production results, and then the influence became slow.

## 2.2 Effect of temperature on biomass gasification

The designed gasification reactor without the structure of the heat source, we cannot control rotary furnace internal temperature through the external heating mode, in order to reduce the influence of other variables, we controlled excess air coefficient of 0.3 by adjusting the primary air and the feed at the same time, keeping the speed of the rotary kiln 3 r/min constant, we obtained the gasification characteristic parameters under different temperature conditions.

Gas composition changed with temperature as shown in Fig. 8, the composition of CO and $H_2$ increased with the increase of temperature, while the $CO_2$ and $CH_4$ concentration was decreased, and the $C_mH_n$ concentration changed little. In the gasification reaction mechanism $C + CO_2 \rightarrow 2CO$ and $C + H_2O \rightarrow CO + H_2$, which are both endothermic reactions, the increasing temperature promotes the gasification reaction rates; while methane formation reaction $C + 2H_2 \rightarrow CH_4$ is an exothermic reaction, temperature has an inhibitory effect on the reaction.

The gas heat value and gas yield changed with

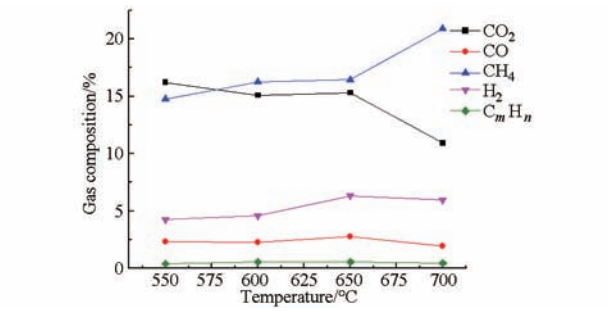


Fig. 8 Variations of gas composition with temperature

temperature as shown in Fig. 9, the heat value obviously increased as the temperature increased, with the increase of temperature, the more gas components were generated from the biomass pyrolysis process, while tar pyrolysis was easy to decompose into gas component at high temperature; on the other hand, carbon dioxide reduction reaction and water gas reaction promoted the increase of fuel gas under high temperature, the gas yield would increase with increasing temperature; heat value and gas yield had a rapid increase and then slowing growth process, it is helpful to the rapid increase of gas heat value and gas yield under the experimental conditions in the range of 600 ~ 650 ℃.

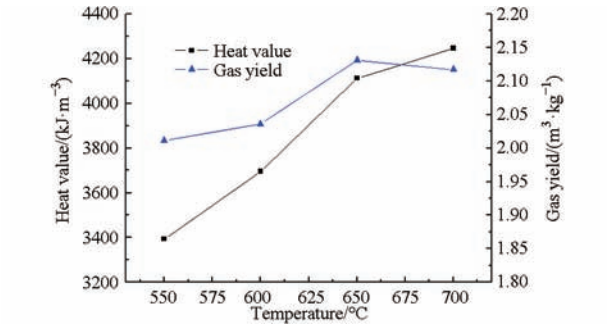


Fig. 9 Variations of gas LHV and gas yield with temperature

Fig. 10 displayed the carbon conversion and gasification efficiency changes with temperature, carbon conversion and gasification efficiency had the increasing trend with the temperature increasing, as to the gasification efficiency was directly related with the heat value and gas yield, and heat value and gas yield increased with the temperature increasing, so the gasification efficiency showed the same change trend, and it was affected larger by the temperature than that of carbon conversion rate; carbon conversion and gas composition and gas yield associated with elevated temperature, as the tar and the carbon in fixed carbon got into the gas phase, the carbon conversion rate increased gradually.

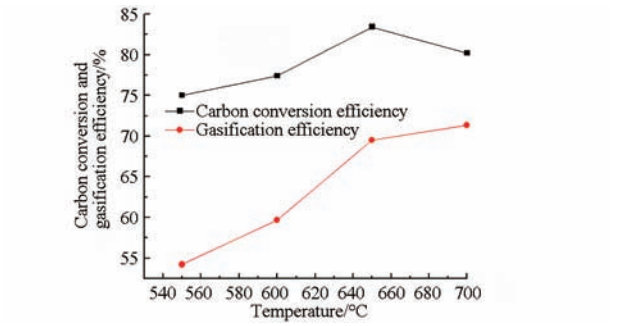


Fig. 10 Variations of carbon conversion efficiency and gasification efficiency with temperature

### 2.3 Effect of equivalence ratio (ER) on biomass gasification

Equivalence ratio in the bed material zone is one of the most important parameters to the gasification process, it has a direct impact on gasification reaction product proportion, and also changed the bed layer temperature indirectly affecting the gas properties. We controlled speed of the rotary kiln constant for 3 r/min, and the measured average temperature of the bed material was about 650 ℃, and it had increasing trend with the increase of equivalence ratio.

Gas composition changed with equivalence ratio as shown in Fig. 11, CO and $H_2$ increased firstly and then decreased, $CO_2$, $CH_4$ and $C_mH_n$ concentration decreased with the increase of equivalence ratio. From Fig. 12, we can see that the gas heat value also experienced increasing firstly and then decreasing process during the change, we got better gas composition and heat value as the equivalence ratio roughly between 0.25 ~ 3, and gas yield had a stable increasing trend with the equivalence ratio increase, the gas heat value rapidly declined with the non-combustible component $N_2$ increasing.

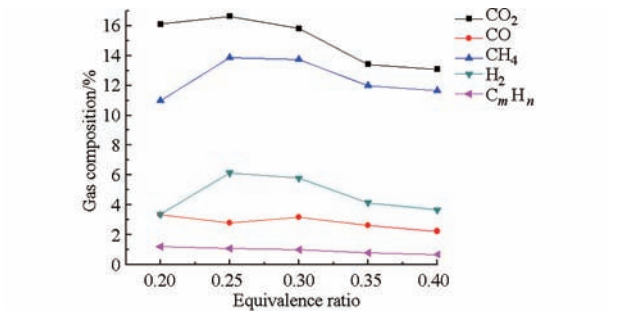


Fig. 11 Variations of gas composition with ER

Carbon conversion and gasification efficiency of the gasification process had relation with the equivalence ratio. As can be seen from Fig. 13, when equivalence ratio was small, the carbon conversion and gasification

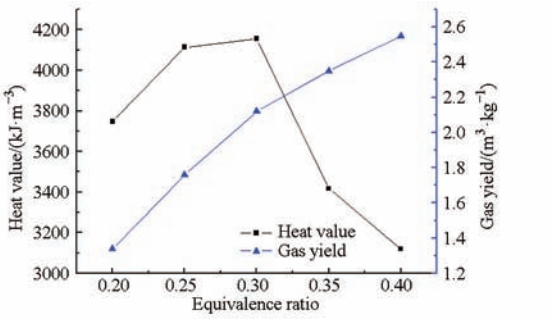


Fig. 12 Variations of gas LHV and gas yield with ER

efficiency increased with the increase of the equivalence ratio, and they peaked when the experiment condition equivalence ratio was 0.3, then the two indicators had declined. Analyze the reasons, the gasification medium involved into the partial combustion, non-combustible components enabled the gas heat value rapidly decreased; the carbon conversion declined due to the gas flow rate increasing, which resulted in carbon emissions increase, and the experimental results was in close to literature [15].

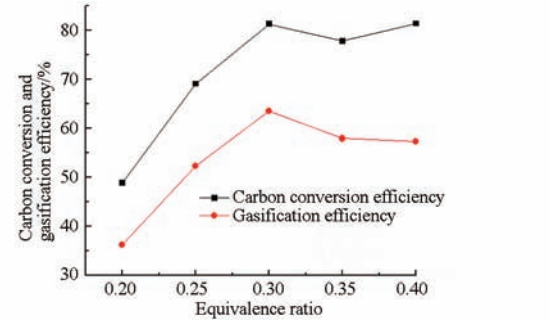


Fig. 13 Variations of carbon conversion efficiency and gasification efficiency with ER

## 2.4 Typical result analysis

In the varying condition experiments, the equivalence ratio changed in the range of 0.2 ~ 0.4, and the operating condition 0.3 was selected as a typical one: the feeding amounted 2.6 kg/h, the speed of the rotary kiln maintained 3 r/min, the average temperature of the material bed zone measuring point was about 700 ℃, the temperature of the bed material zone is relatively uniform when the rotary kiln speed was large; the temperature of the upper portion of the rotary kiln was about 570 ℃, because of the fuel heating, drying and pyrolysis process, which made the temperature here below the bed material zone. The gasification reactor product gas was led into the secondary combustor, the location of the thermocouples from bottom to the upper part of the combustor was 300 mm, 700 mm, 1 000 mm, the monitoring temperatures were about 924 ℃, 1 000 ℃, 840 ℃, and the secondary combustion chamber burn emissions in flue gas volume fraction of CO was about $1.5 \times 10^{-4}$ ~ $2.0 \times 10^{-4}$, volume fraction of $NO_x$ was about $2.0 \times 10^{-4}$ ~ $4.0 \times 10^{-4}$.

### 2.4.1 Gas analysis

The fuel gas under stable gasification condition was collected, and we used gas chromatography to analyze gas composition, the results were in comparison with the bubbling fluidized bed and circulating fluidized bed biomass gasification typical gas components, as shown in Tab. 1. The results of the rotary gasification reactor were similar with the fluidized-bed. To some degree, it can be seen as a special fluidized bed gasifier, except that by using the mechanical perturbation instead of flow of air, Since it is unnecessary to consider the coordination between primary air and the fluidized bed material particles, we have greater flexibility in the regulation.

**Tab. 1 Gas composition of rotary gasifier under typical operation condition**

| Furnace | Gas composition/% | | | | | | |
|---|---|---|---|---|---|---|---|
| | CO | $CO_2$ | $H_2$ | $CH_4$ | $C_mH_n$ | $N_2$ | $O_2$ |
| Rotary gasifier | 13.75 | 15.82 | 5.51 | 3.17 | 0.99 | 58.77 | 0.93 |
| Bubbling fluidized bed gasifier[22] | 13 ~ 16 | 10 ~ 14 | 4 ~ 8 | 3 ~ 7 | 1.5 ~ 2.9 | 45 ~ 55 | 0.8 ~ 2 |
| Circulating fluidized bed gasifier[22] | 14 ~ 23 | 7 ~ 15 | 4 ~ 8 | 4 ~ 10 | 1 ~ 2.5 | 45 ~ 60 | 0.8 ~ 2 |

According to the quantitative evaluation parameters of the rotary gasification reactor, Carbon conversion efficiency is the share of carbon from biomass fuel converted into gas fuel, calculated as follow[20]:

$$\eta_c = \frac{M_{CH_xO_y}(C_{CO} + C_{CO_2} + C_{CH_4} + 2.5C_{C_mH_n})}{22.4} G_y$$

In the formula, $C_{CO}$, $C_{CO_2}$, $C_{CH_4}$, $C_{C_mH_n}$ represent the corresponding gas volume fraction in the gasification gas respectively, $M_{CH_xO_y}$ refers to the molecular weight of the biomass characteristics formula, it is obtained from the simplified proportion of elemental analysis of the biomass. In this study, the molecular

characteristics of biomass was $CH_{1.5}O_{0.68}$ and characterizing molecular weight was about 24.4, calculated carbon conversion efficiency was 81.3%; calculation of the gas yield was about 2.1 $m^3/kg$; at the same time, the gasifier gasification efficiency was about 64.3%, and considering the sensible enthalpy it was about 79.3%.

Typical experimental results showed that the gas heat value was about 4 156 $kJ/m^3$ with air as the gasifying medium, and it was relatively low mainly due to tar was not included in the product gas, as it was condensed and removed during the measurement process of the product gas, and heat loss of the small experimental equipment was also one of the major reasons.

### 2.4.2 Energy balance analysis

Energy balance of the characteristics of the experimental system is also a measure indicator of the gasification combustion apparatus; we can determine the distribution of the various parts of the system energy flow by energy balance calculation, by calculating the energy conversion efficiency and heat loss, it provided data support to improve the efficiency of the reaction[23].

The energy into the system is equal to the sum of the energy leaving the system when the experimental system of the gasification process was in steady conditions, the specific energy flow is shown in Fig. 14, and energy in the figure is corresponded to per unit mass of fuel. Fuel and gasification medium in the system carried energy into the gasifier, including heat losses and residual carbon losses in gasifier, as well as energy in the hot gas $Q_g$, chemical energy in the tar $Q_{Tar}$ and sensible heat $Q_H$. Tar and hot gas carried energy into the secondary combustion chamber, to achieve complete conversion process from chemical energy to flue gas sensible heat, which took full advantage of tar and fuel gas sensible heat.

Since tar and hot gas are both used as fuel into the secondary combustion chamber, the gasifier was a core part of the energy conversion system, and the energy balance equation as follow:

$$Q_{ar} + Q_m = Q_g + Q_H + Q_{Tar} + Q_r + Q_c$$

The energy calculation methods of each part are shown in literature [22], with the standard environment as the background, results as shown in Tab. 2.

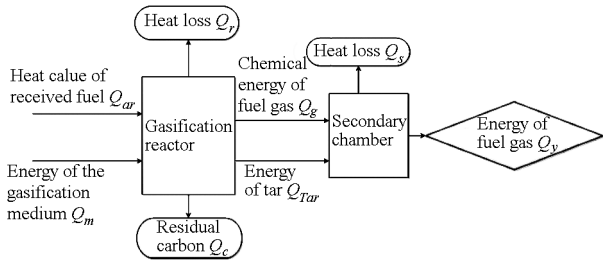


Fig. 14 Energy balance system of experiment

**Tab. 2 Energy balance results of gasification system**

| | Project | Energy/kJ | Proportion/% |
|---|---|---|---|
| Input energy | $Q_{ar}$ | 13 724 | 95.5 |
| | $Q_m$ | 643 | 4.5 |
| Effective energy | $Q_g$ | 8 830 | 61.5 |
| | $Q_H$ | 2 150 | 15.0 |
| | $Q_{Tar}$ | 1 494 | 10.4 |
| | Total | 12 474 | 86.8 |
| Energy loss | $Q_r$ | 1 565 | 10.4 |
| | $Q_c$ | 329 | 2.8 |
| | Total | 1 894 | 13.2 |

The energy balance results with gasifier as the core are shown in Tab. 2, in which effective energy accounted for 86.8% of the total input, heat loss $Q_r$ accounted for 13.2% of the total energy losses as the main energy loss, insulation performance of the small experimental equipment could be improved.

### 2.4.3 Distribution of bottom ash analysis

Gas-solid phase reaction of semi-coke in reactor is the main process of biomass gasification, analysis of bottom ash and semi-coke particle morphology is helpful to understand the operating characteristics of the gasification reactor.

At the end of the stable operating conditions, bottom ash and bed material was separated by a porous mesh, since the bed material diameter is in 3 ~ 5 mm range, mesh diameters in four kinds 2.5 mm, 1.25 mm, 0.5 mm, 0.3 mm are chosen for bottom ash separation, bottom ash particle morphology of different sizes is shown in Fig. 15. Among them, left four images respectively corresponded to four separated bottom ash, the upper right corner shows char particle image in the gasifier, the lower right corner shows the bed material and char mixing state.

As can be seen from Fig. 15, bottom ash form distribution shows that there was no obvious bottom ash slagging under mechanical disturbance and bed

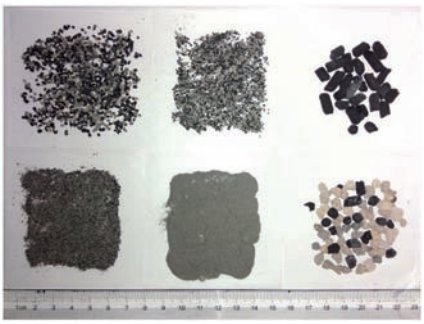

Fig. 15 Bottom ash morphology of different particle sizes

material mean temperature effect. Sample on the right side is the char and bed material mixture, wherein the surface of the char particles had little ash, char and bed material were relatively homogeneous mixing in the furnace. Experimental results show that char particles and the bed material had good mixing characteristics in the bed material zone.

In order to analyze the distribution of biomass ash in the rotary furnace quantitatively, the bed material was divided into two average parts according to the upper and lower positions, then separated and weighed the ash respectively, the results are shown in Tab. 3.

**Tab. 3 Bottom ash distribution in bed material area**

| Mass distribution/g | Particle diameter distribution/mm | | | |
|---|---|---|---|---|
| | 0 ~ 0.3 | 0.3 ~ 0.5 | 0.5 ~ 1.2 | 1.2 ~ 2.5 |
| Upper zone | 90.0 | 23.6 | 20.4 | 18.0 |
| Lower zone | 1087.5 | 328.2 | 152.6 | 87.4 |

As seen from Tab. 3, the small size ash particles in bed material zone accounted for the main ash, the particle size in the bottom ash below 0.5 mm accounted for 85% of the total mass. On the other hand, according to the stratified sampling results, bottom ash distribution mainly concentrated in lower part of the bed material zone and accounting for more than 90% of the total mass of bottom ash, which has reference to the bed material and bottom ash separation, and slag discharging outlet design.

## 3 Conclusions

(1) With biomass particles as raw materials, the rotary gasifying reactor realized the partial air gasification, and it can be in good control of gasification temperature in the reaction zone, to ensure the smooth progress of the gasification process, at the same time, the product gas can complete the process of staged combustion in the subsequent secondary combustion chamber.

(2) The experimental results show that the rotating speed affects the mixed disturbance characteristics and the temperature distribution in the furnace, and then it has an important influence on the characteristic parameters of the biomass gasification reaction. In the experiment range, with the increase of rotary speed, the combustible gas heat value, gas yield, carbon conversion and gasification efficiency were increased, it got good gas production results as the speed of the rotary kiln was 3 r/min, then the influence degree became slow.

(3) In the experiment we controlled the temperature in the range of 550 ~ 700℃, the gasification parameters increased with temperature increasing, the gas heat value and gasification efficiency were effected more by temperature. Under experimental conditions in 600 ~ 650℃ temperature range the heat value of the combustible gas and the gasification efficiency and other indicators had greatly improved.

(4) The equivalent ratio changed in the range of 0.2 ~ 0.4, and it had a greater impact on gas production results of the indicators, with the increase of equivalence ratio, the gas production rate and bed temperature increased to a certain degree, the change trend of other gasification index parameters are first increased and then decreased, we got the better gasification results with ER of 0.3.

(5) The typical result shows that the gas composition of the rotary gasifier is close to that of the fluidized bed, considering the sensible enthalpy, the gasification efficiency is about 77.9% and the carbon conversion rate is about 81.3%. The gasifier energy balance is calculated, and the output efficiency of the system is 86.8%, with the heat dissipation as the main energy loss way.

(6) The separation of the bottom ash with bed material find that about 86% of the total ash content remain in the bed material area, and more than 90% of them are distributed in the bottom of the bed material area. Experimental results are optimized by controlling the variables for the operation and design of the new type of gasifier improvement to provide reference.

**References**


[1] YANG Qian, ZENG Lingke. Status and characteristics of the domestic furnace[J]. Ceramics, 2010(2): 44 - 49. (in Chinese)

[2] CHI Yong, ZHANG Zhixiao, YAN Dahai, et al. Movement and heat transfer modeling of tire pyrolysis in a rotary kiln[J]. Journal of Engineering Thermophysics, 2004, 25(2): 333 - 336. (in Chinese)

[3] LI Qingshui, CHI Yong, LI Rundong, et al. Municipal solid waste rotary kiln incinerator design with respect to 3T principles[J]. Power Engineering, 2002, 22(5): 1983 - 1989. (in Chinese)

[4] MA Jianlu, YANG Chuanfang. Controlling of operation of sludge rotary incinerator[J]. Industrial Water & Wastewater, 2003, 34(1): 68 - 70. (in Chinese)

[5] WEN Shien, CHI Yong, ZHANG Zhixiao, et al. Study on characteristics of pyrolytic char from pyrolysis of scrap tires in a pilot-scale rotary kiln[J]. Journal of Combustion Science and Technology, 2003, 9(2): 186 - 189. (in Chinese)

[6] ZHANG Zhixiao. Investigation of waste tire pyrolysis in rotary kiln and the application project[D]. Hangzhou: Zhejiang University, 2004. (in Chinese)

[7] CHEN Wenzhong, WANG Chunhua, TIAN Yuanhang, et al. Numerical simulation on influence factors of thermal working conditions in carbon rotary kilns[J]. Journal of Chemical Industry and Engineering (China), 2011, 62(1): 47 - 52. (in Chinese)

[8] YANG Hua, CHEN Quanming, XUE Dongwei, et al. Innovative design on waste rotary kiln incinerators[J]. Machinery, 2004, 31(2): 48 - 49. (in Chinese)

[9] ELATTAR H F, STANEV Rayko, SPECHT Eckehard, et al. CFD simulation of confined non-premixed jet flames in rotory kilns for gaseous fuels[J]. Computers Fluids, 2014, 102: 62 - 73.

[10] HERZ F, MITOV I, SPECHT E, et al. Influence of the motion behavior on the contact heat transfer between the covered wall and solid bed in rotary kilns[J]. Experimental Heat Transfer, 2015, 28(2): 174 - 188.

[11] THAMMABONG Phahath, DEBACQ Marie, VITU Stéphane, et al. Experimental apparatus for studying heat transfer in externally heated rotary kilns[J]. Chemical Engineering Technology, 2011, 34(5): 707 - 717.

[12] WANG Chunliang. Analysis of the development of circulating fluidized bed at home and abroad[J]. Energy Conservation Technology, 2011, 29(2): 143 - 144. (in Chinese)

[13] XIAN Jianwei, FAN Xiaoxu, HAN Zhonghe, et al. Effects of the bed material on biomass gasification in fluidized bed gasifier[J]. Renewable Energy, 2011, 29(1): 45 - 48. (in Chinese)

[14] FAN Xiaoxu, XIAN Jianwei, CHU Leizhe, et al. Comparison of bubbling fluidized bed and circulating fluidized bed in gasification of biomass[J]. Transactions of the Chinese Society for Agricultural Machinery, 2011, 42(4): 96 - 99. (in Chinese)

[15] XIE Jun, WU Chuangzhi, CHEN Ping, et al. An experimental study on biomass gasification in a medium fluidized bed gasifier[J]. Acta Energiae Solaris Sinica, 2007, 28(1): 86 - 90. (in Chinese)

[16] GAI Chao, DONG Yuping. Temperature distribution and gas composition of biomass gasification in downdraft fixed bed gasifier[J]. Transactions of the Chinese Society for Agricultural Machinery, 2012, 43(5): 91 - 96. (in Chinese)

[17] YAO Zonglu, MENG Haibo, TIAN Yishui, et al. Design and experiment on anti-slagging biomass pellet fuel burner[J]. Transactions of the Chinese Society for Agricultural Machinery, 2010, 41(11): 89 - 93. (in Chinese)

[18] TAN Li. Study on then alkali transformation behavior and slagging characteristics during biomass combustion[D]. Beijing: North China Electric Power University, 2014. (in Chinese)

[19] HUANG Fang. Study on the deposit and corrosion problem on heating surface during straw combustion[D]. Hangzhou: Zhengjiang University, 2013. (in Chinese)

[20] ZANG Yunhao, LIU Yunquan, WANG Duo, et al. Study on gasification performance of a two-stage downdraft gasifier[J]. Renewable Energy Resources, 2014, 32(6): 836 - 841. (in Chinese)

[21] PAN Xianqi, SU Deren, ZHOU Zhaoqiu, et al. Experimental investigation of biomass gasification in a pilot-scale fluidized bed gasifier[J]. Transactions of the Chinese Society for Agricultural Machinery, 2014, 45(10): 175 - 179. (in Chinese)

[22] SUN Li, ZHANG Xiaodong. Biomass pyrolysis gasification principle and technology[M]. Beijing: Chemical Industry Press, 2012. (in Chinese)

[23] CHU Leizhe, FAN Xiaoxu, XIAO Qi, et al. Dual fluidized bed biomass decoupled gasification experiments[J]. Transactions of the Chinese Society for Agricultural Machinery, 2010, 41(Supp.): 117 - 120. (in Chinese)

[24] LAI Xirui, ZHOU Zhaoqiu, LIU Huacai, et al. Experiment study of biomass ash sintering and melting[J]. Transactions of the Chinese Society for Agricultural Machinery, 2016, 47(3): 158 - 166. (in Chinese)

[25] YAO Zonglu, WU Tongjie, ZHAO Lixin, et al. Design and experiment of flue gas dilution sampler for biomass fixed combustion source[J]. Transactions of the Chinese Society for Agricultural Machinery, 2016, 47(3): 174 - 178. (in Chinese)

[26] YAO Xiwen, XU Kaili, XU Xiaohu. Influence of ashing temperature on slagging and fouling characteristics of biomass ash[J]. Transactions of the Chinese Society for Agricultural Machinery, 2016, 47(1): 182 - 189. (in Chinese)

doi:10.6041/j.issn.1000-1298.2016.06.027

# 含床料的回转式生物质气化反应器实验

余春江　翟相和　解桂林　周宇盛　涂汉超
（浙江大学能源清洁利用国家重点实验室，杭州 310027）

**摘要**：为将传统回转炉窑机械扰动特性与流态化反应器内惰性床料的均温蓄热特性相结合，提出一种回转式气化反应器设计模式，以棉秆颗粒燃料为实验原料，首先考察了回转炉转速、过量空气系数、温度等参数对气化反应系统的影响。实验结果表明，回转炉转速控制在 1～4 r/min 之间，随转速增加回转炉混合扰动特性增强，炉内温度分布更加均匀，不同指标参量均有提高，在实验范围内回转炉转速在 3 r/min 时，取得较好的产气结果；实验控制温度在 550～700℃范围，各指标均随温度升高有增大趋势，其中燃气热值、气化效率受温度影响较大，实验条件下，600～650℃温度范围内燃气热值和气化效率等指标有较大提升；过量空气系数对产气结果的各项指标均有较大影响，实验控制过量空气系数在 0.2～0.4 范围内变动，随过量空气系数增加，除产气率和床料区温度在一定程度增大外，其他指标均有先增大后减小的变化趋势，实验中过量空气系数为 0.3 时气化效果较好。典型热态实验结果表明，该回转式气化反应器产出的燃气组分与流化床接近，考虑显焓的气化效率约为 79.3%、碳转化率约为 81.3%；以气化炉为核心进行能量平衡计算，显示系统有效输出效率达到 86.8%，散热损失为主要能量损失途径；对床料区底灰的分离研究发现，床料区滞留的底灰超过 90% 停留在床料区下部，且大部分底灰粒径较小。通过控制变量得到优化实验结果，可为该炉型的运行和设计改进提供参考。

**关键词**：回转式气化反应器；床料；生物质；气化效率
**中图分类号**：TK6　　**文献标识码**：A　　**文章编号**：1000-1298(2016)06-0207-08

# Experiment on Biomass Rotary Gasifier with Bed Material

Yu Chunjiang　Zhai Xianghe　Xie Guilin　Zhou Yusheng　Tu Hanchao
(*State Key Laboratory of Clean Energy Utilization*, *Zhejiang University*, *Hangzhou* 310027, *China*)

**Abstract**: In order to combine the traditional rotary mechanical disturbance characteristic with the inert bed material heat storage properties, a new type of rotary gasifier was designed. On the basis of the new type of rotary gasifier, a staged gasification and combustion experimental platform was designed and the thermal state test of the system was completed. The effects of rotational speed, equivalence ratio, temperature and other parameters on the gasification reaction system were investigated. The experimental results showed that when rotary furnace speed was controlled at 1～4 r/min, the rotary furnace mixed disturbance characteristics were enhanced with the increase of rotary speed, and temperature distribution was more uniform in the furnace, different parameters were improved in the experimental range, good gas production was got at rotary furnace speed of 3 r/min. When temperature was controlled in the range of 550～700℃, the gasification parameters were increased with the increase of temperature, and gas calorific value and gasification efficiency were affected greatly by temperature. Under the experimental conditions with temperature of 600～650℃, the calorific value of combustible gas, gasification efficiency and other indicators were greatly improved. The equivalent ratio (ER) was changed in the range of 0.2～0.4, and it had great impact on gas production of the indicators, with the increase of equivalence ratio, the gas production rate and bed temperature were increased to a certain degree, the change trend of

收稿日期：2016－01－06　修回日期：2016－01－31
**基金项目**：国家自然科学基金项目(51336008)
**作者简介**：余春江(1973—)，男，教授，主要从事生物质能热化学转化和煤炭清洁高效利用技术研究，E-mail：chunjiang@zju.edu.cn

other gasification parameters were firstly increased and then decreased, good gasification results were obtained with ER of 0.3. The typical result showed that gas composition of rotary gasifier was close to that of the fluidized bed, considering the sensible enthalpy, the gasification efficiency was about 79.3% and the carbon conversion rate was about 81.3%. The gasifier energy balance was calculated, and the output efficiency of the system was 86.8%, with heat dissipation as main energy loss way. It was found from the separation of the bottom ash with bed material that about 86% of the total ash content was remained in the bed material area, and more than 90% of it was distributed in the bottom of the bed material area. Experimental results were optimized by controlling the variables for operation and design of new type of gasifier improvement to provide reference.

**Key words**: rotary type gasifier; bed material; biomass; gasification efficiency

## 引言

传统回转炉主要用于粉料或者矿物材料的初级加工行业[1]。由于回转炉本身对物料形状、尺寸适应性强,炉内的机械扰动可促进物料充分混合以及传热[2-3]。近 30 年来,国内外研究学者针对回转炉型在废弃物焚烧领域展开一系列研究,主要针对污泥、医疗废弃物等低热值固体废弃物的热解焚烧处理[4-11]。

传统的回转炉焚烧炉内参与反应的是固体物料和用于燃烧的空气,物料在炉体旋转运动下被带动并逐渐从炉体的一端运动到另一端并在期间与空气接触完成燃尽。为了增加对炉内物料热化学反应温度的可控性并进一步强化物料气固相反应涉及的传热传质过程,参考流态化反应条件,在反应体系中加入热容量较大的惰性床料颗粒是可行的途径[12-13]。为此要对常规回转炉进行改进,使炉体内能够蓄积较大量的惰性床料,并利用炉体的回转运动带动床料颗粒运动,替代流化床中流化风的流化作用实现回转炉内部扰动混合。本文通过探究气化炉机械扰动特性对流化介质与物料反应的影响,验证该改进型回转反应器应用于对转化过程温度控制较为严格的高碱类生物质原料的气化或者燃烧过程的可行性。

## 1 实验方案

### 1.1 气化装置结构特点

为了验证该新型回转式气化反应器的适用性和气化性能,进行了生物质成型燃料的部分空气气化方案设计[14-16]。考虑到需要在回转反应器内蓄积床料,一种比较简单的方案就是增加筒体的布置倾角,采用较低的长径比,封闭筒体底端,如图 1 所示。在该方案中,惰性颗粒状床料在反应器中下部蓄积并在筒体回转过程中被筒壁携带受到充分扰动。空气作为气化介质在筒体底端一次风入口引入床料区域,燃料通过布置在上部气相空间的给料口给入到床料区域,与高温床料均匀混合发生干燥和热解,并与通入床料区域的空气接触完成部分燃烧和气化反应。产品气经由设置在气相空间的排烟口引出反应器。反应器还设置有常规的支撑和回转驱动装置以确保反应器本体能稳定地以设定转速回转运动。

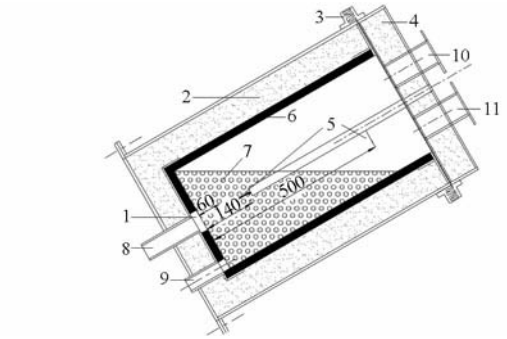


图 1 新型回转式气化炉实验结构图

Fig. 1 Schematic diagram of new rotary gasifier

1. 多孔布风板 2. 保温层 3. 迷宫式轴向密封环 4. 固定顶盖 5. 热电偶 6. 高温耐火材料 7. 床料区 8. 一次风入口 9. 排渣口 10. 给料口 11. 产品气引出口

实验设计回转式气化反应器保留了传统回转炉机械扰动以及调控便利的优点,并通过床料介质的引入强化了物料颗粒周边传热传质过程,对于生物质而言,床料与原料颗粒的相互扰动可剥离颗粒表面灰层,促进半焦颗粒破碎离析,大幅度促进气化反应进程。另一方面,较小的长径比设计以及惰性床料稳定地留存于反应器内部的设计思路提升了反应器空间的利用率,易于确保物料的反应时间并提高气固相反应效率,在设备占地和制造成本方面有较大优势。

与传统回转炉相比,反应器内惰性床料热容量大,有利于控制并维持反应区温度,这对于气化燃烧过程中需要严格控制反应温度具备底灰熔点的生物质原料而言具有重要意义[17-19];此外反应器内较大的热容量也有利于提高原料适应性,增加设备应对原料特性波动的能力。该气化装置在高碱生物质颗

粒气化或分级燃烧领域有推广应用的潜力，可以较好地应对碱金属沉积结渣以及燃烧过程氮氧化物控制等问题。

### 1.2　实验方案设计

为了研究该回转式生物质气化装置性能特点，进行了相关的实验台设计搭建。验证实验的回转炉气化装置如图 1 所示，反应器主体包括可进行回转运动的回转炉体以及图 1 中部件 4 所描述的固定顶盖两部分，二者之间由迷宫式轴向密封环连接。

实验中采用的回转反应器长径比约为 2.1，旋转轴线倾角与水平方向呈 30°布置，床料选用粒径约 3 ~ 5 mm 的石英砂颗粒；气化所用空气由一次风引入口通过多孔板进入反应器内床料所在空间，孔径大致 1 mm，以防止床料泄露损失；反应器外层为钢板，内壁为耐磨浇注料，其间设置 80 mm 保温材料，以确保反应器为绝热设计；反应器底部的排渣口设计有孔径 1 mm 的多孔板挡板以便在排出灰分的同时将床料保留在反应器内。反应器顶盖上设置有测温热电偶保护套管，内置热电偶分别监测床料区底部、上部空间以及引出的产品气温度。

图 2 为实验装置三维结构示意图，给出了反应器本体的密封、驱动和支撑方案的部分具体结构。如图所示，回转炉本体由 4 个托轮支撑回转，回转炉体上固定齿圈，与减速机小齿轮啮合驱动，减速机配套电机可变频调速，炉体转速调节在 2 ~ 6 r/min 之间；反应器顶盖安装在固定支撑轴上，可沿轴向移动，方便顶盖的开闭、床料的更换以及内部清灰检修等操作。

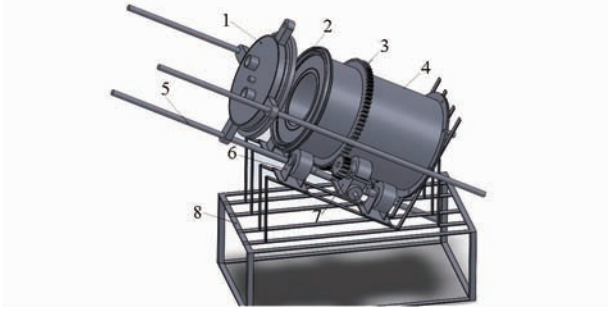


图 2　回转式气化炉立体效果图

Fig. 2　Stereoscopic effect diagram of rotary gasifier

1. 顶盖　2. 迷宫式轴向密封环　3. 齿圈　4. 回转炉体　5. 顶盖支撑轴　6. 托轮　7. 减速机　8. 底部支架

### 1.3　热态实验

#### 1.3.1　燃料特性

实验采用棒状棉秆颗粒燃料，原料颗粒直径 4 mm，长度约 10 mm，工业、元素分析显示，燃料热值约为 13.7 MJ/kg；实验燃料中挥发分组分比例最大，质量分数约 63%，灰分含量最少，质量分数约为 7%，且元素组成中 C 与 O 含量最大，质量分数分别占总量的 41% 和 37%，说明棉秆颗粒燃料具备常规生物质高挥发分、高氧含量的特点。

燃料灰成分显示，$SiO_2$ 与 CaO 为灰分的主要组成，二者质量分数将近灰分的 50%，同时 $K_2O$ 与 $Na_2O$ 占灰成分的 12%，灰成分体现了典型的草本农业生物质特性，实验燃料中较高的 K、Na 含量使热化学反应过程中容易诱发结渣、沉积等碱金属问题，需要比较严格地控制反应过程温度。

#### 1.3.2　实验系统

图 3 为回转式生物质气化反应器热态实验系统，该系统是一个生物质颗粒分级燃烧装置，生物质颗粒回转式气化反应器中进行部分空气气化，产生的产品气进入气体燃烧装置进行燃烧，完成生物质颗粒燃烧转化利用。由于气化过程的温度可以得到很好控制，因而该技术可以适用于灰熔点很低的农作物秸秆制备的颗粒燃料；此外气化装置产生燃气可以比较容易地通过燃烧组织实现低氮排放，该工艺路线对于小规模生物质成型燃料燃烧利用具有较高的推广应用价值。

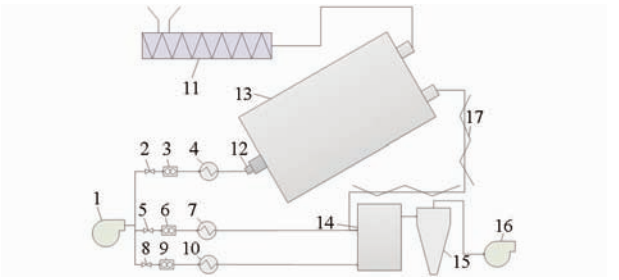


图 3　回转式生物质气化炉实验系统原理图

Fig. 3　Experimental system diagram of biomass rotary gasifier

1. 鼓风机　2. 气化给风阀门　3、6、9. 转子流量计　4、7、10. 预热器　5. 二燃室一次风阀门　8. 二燃室二次风阀门　11. 给料机　12. 旋转接头　13. 回转炉本体　14. 燃气燃烧设备　15. 旋风分离器　16. 引风机　17. 保温加热设备

实验系统包括给风装置，依次有鼓风机、阀门、转子流量计以及预热器等，提供 300℃左右的气化给风作为回转气化炉气化介质；给料装置可通过变频器调节给料量，可以稳定供给棉秆颗粒燃料；回转炉主体完成颗粒燃料的气化过程，产生的燃气进入燃气燃烧装置燃尽。系统还包括旋风分离器、引风机以及辅助的空气预热、测试和取样系统等。

生物质气化中焦油处理问题是常规气化应用中必须考虑解决的问题，实验中采用分级燃烧方式，燃气与焦油均可在二燃室高温条件下得到利用。因此，实验中要保证焦油通过气化炉与二燃室的中间管路不凝结，如图 3 所示，在该段管路设置保温加热

设备,控制管路温度在300℃以上以满足条件。

### 1.4 实验方法

实验中通过直接加热床料的方式进行预热,然后将温度在400℃左右的床料转移至回转炉内部,加入点燃的煤炭进行升温,待温度升高到550℃附近时,调节给料量与一次风量,待工况稳定后开始采样测量,每个工况采样3次,以减少实验误差。实验中需要调整控制的变量包括回转炉转速、过量空气系数以及气化炉内部温度3个变量,为此分别研究3种变量对气化炉性能指标等参数的影响。

本文中采用产气热值、气体产率、气化效率、碳转化率4种状态参数表征回转炉运行状态以及对气化效果评估,具体计算方法参照文献[15,20]。

### 1.5 采样与测试

采样过程将气体通过蛇形管以及洗气瓶等在低温环境(-10℃)下冷却除去焦油,用集气袋收集气体后,用Agilent 7890A GC型气相色谱离线分析气体样品组分,主要确定气体中的CO、$CO_2$、$H_2$、$CH_4$、$N_2$、$C_mH_n$等气体组分[21]。

## 2 结果与讨论

### 2.1 回转炉转速对生物质气化的影响

回转炉转速直接影响回转炉内部的温度分布、物料以及气化介质的混合扰动程度,从而对产气效果有较大影响。实验中,回转炉转速对炉内温度分布影响随时间变化过程如图4所示。

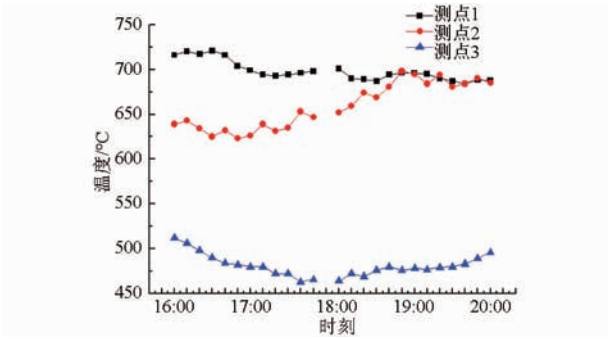


图4 回转炉轴向温度随时间的变化曲线

Fig. 4 Variation curves of axial temperature of rotary furnace with time

从图4可以看出,由16:00进入工况开始,由于给料上的波动,回转炉内部温度也有一定变化,2个测点之间相差50℃,但床料区温度总体变化不大,相对较为稳定;在断点(17:50)位置回转炉转速由2 r/min增加到3 r/min,改变转速后,床料区温度出现较为明显变动,其中测点1和测点2的温度向中间靠拢,随后温差减小直至趋于稳定。因此,回转炉内部床料区温度随转速增大温度趋于均匀,且波动幅度减小,上部空间温度随转速增加有增大趋势,从温度变化上体现了回转炉的转动过程对于物料混合反应的促进效果。

燃气组分随转速变化见图5,不同可燃气组分随转速增加有增大趋势,整体变化趋势相对稳定;其中$CO_2$、$H_2$以及CO等产气成分随转速变化趋势明显。

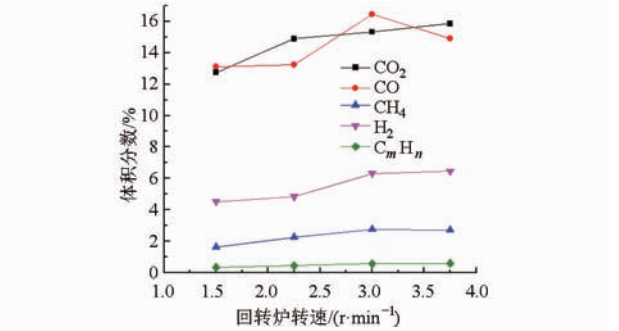


图5 气体组分随转速的变化曲线

Fig. 5 Variation curves of gas composition with rotary speed

回转炉转速增加,回转炉床料区温度趋于均匀,且混合效应增强,对于生物质热解产气过程具有促进作用;同时,生物质进入回转炉干燥过程析出水分,转速较低时水分大部分随燃气组分排出,随转速增加部分水蒸气作为气化介质与物料混合反应,$CO + H_2O \rightarrow CO_2 + H_2$的水蒸气重整反应加强,有利于燃气中$CO_2$、$H_2$组分增加。

热值和产气率随转速变化如图6所示,由于床料区温度趋于均匀以及混合扰动的增强,该区域内的气化反应随转速的增大而得到显著增强,以燃气热值以及产气率为特征参量的指标随转速增加而增大;碳转化率以及气化效率随转速变化有相似的变化趋势如图7所示。

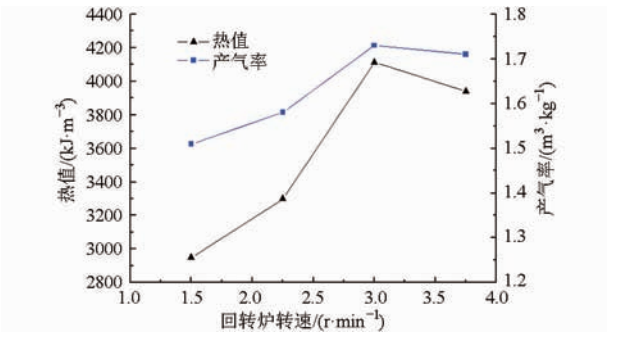


图6 热值和产气率随转速的变化曲线

Fig. 6 Variation curves of gas LHV and gas yield with rotary speed

综合分析,回转炉转速提高影响回转炉混合扰动特性以及炉内温度分布,进而对生物质气化反应的特征参量具有重要影响。且在一定范围内随转速增大,燃气热值、产气率、气化效率以及碳转化率均有提高,在实验中,回转炉转速在3 r/min时,取得较好的产气结果,随后影响程度减缓。

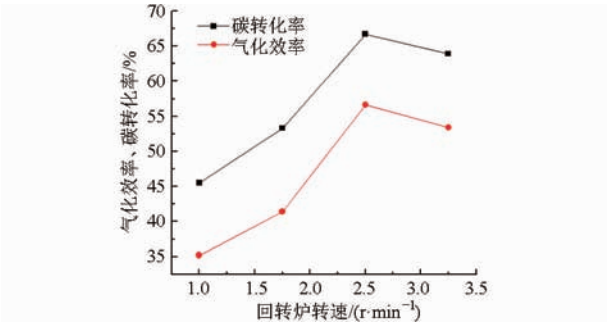


图 7　碳转化率与气化效率随转速的变化曲线

Fig. 7　Variations of carbon conversion efficiency and gasification efficiency with rotary speed

## 2.2　温度对生物质气化的影响

实验中气化反应器无外热源的结构设计，无法通过外部加热方式调控回转炉内部温度，为减少其他变量的影响，采用同时调节一次风量以及给料量的方式，控制过量空气系数维持 0.3 时，选择回转炉转速 3 r/min 恒定，得到不同温度工况下燃气成分以及气化炉的特征参数。

燃气成分随温度的变化如图 8 所示，组分中 CO 与 $H_2$ 均随温度升高而增大，而 $CO_2$ 与 $CH_4$ 含量均有减小，而 $C_mH_n$ 浓度变化不大。气化反应机理中 $C + CO_2 \rightarrow 2CO$ 的二氧化碳还原反应以及 $C + H_2O \rightarrow CO + H_2$ 的水蒸气置换反应均为吸热反应，温度升高使反应速率增大的同时，对上述 2 个反应均有促进作用；而 $C + 2H_2 \rightarrow CH_4$ 的甲烷生成反应为放热反应，温度升高对该反应有抑制作用。

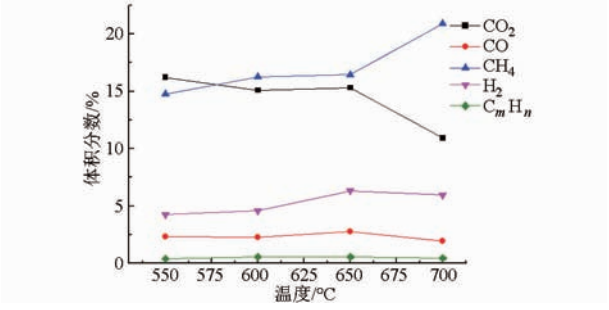


图 8　燃气组分随温度的变化曲线

Fig. 8　Variations of gas composition with temperature

燃气热值与产气率随温度变化曲线如图 9 所示，燃气热值随温度升高而明显增大，温度的升高，使生物质热解过程生成的可燃气组分增大，同时热解生成的焦油在高温条件下易于分解而转变为燃气组分；另一方面，高温条件下的二氧化碳还原反应以及水煤气反应均使可燃气的气体体积增大，产气率也随着温度升高有增大趋势；同时热值和产气率增大过程有一个快速增加而后增幅放缓的过程，实验条件下 600 ~ 650℃ 温度范围内提高温度有助于快速提高燃气热值和产气率。

图 10 为实验过程气化效率和碳转化率随温度

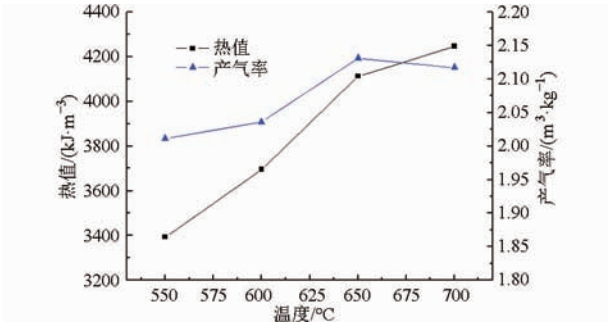


图 9　燃气热值与产气率随温度的变化曲线

Fig. 9　Variations of gas LHV and gas yield with temperature

变化关系图，气化效率和碳转化率均随温度升高有增大趋势，而气化效率受温度的影响明显大于碳转化率，气化效率与燃气的热值以及产气率直接相关，由图 10 分析结果可知，热值与产气率均随温度升高而增大，与这两者均有正相关关联的气化效率表现出同样的变化趋势；碳转化率与燃气成分以及产气率均有关联，随温度升高，焦油以及固定碳中的部分碳元素进入气相，使碳转化率逐渐增大，表现为碳转化率与产气率也有较为相似的变化趋势。

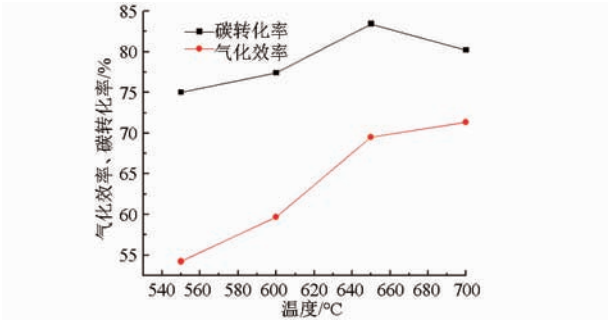


图 10　碳转化率和气化效率随温度的变化曲线

Fig. 10　Variations of carbon conversion efficiency and gasification efficiency with temperature

## 2.3　过量空气系数对生物质气化的影响

回转炉床料层的过量空气系数作为气化过程的重要参数之一，直接影响气化反应产物比例，还改变床层温度间接影响燃气特性。实验中控制回转炉转速恒定为 3 r/min 不变，床料区平均温度约 650℃，随过量空气系数的波动，实验范围内床料区的测点平均温度均随过量空气系数的增大而有增大趋势。

燃气成分随过量空气系数的变化关系如图 11 所示，随过量空气系数增大 CO、$H_2$ 等可燃气组分先增大后减小，$CO_2$、$CH_4$ 以及 $C_mH_n$ 含量有减小趋势。从图 12 中可以看出，燃气热值同样经历了先增大后减小的变化过程，过量空气系数大致在 0.25 ~ 0.3 之间时有较好的燃气组分以及燃气热值，而产气率随过量空气系数的增大呈稳定增大趋势，而非可燃组分 $N_2$ 等气体成分的增多使燃气热值快速下降。

生物质气化反应中，气化效率以及碳转化率同

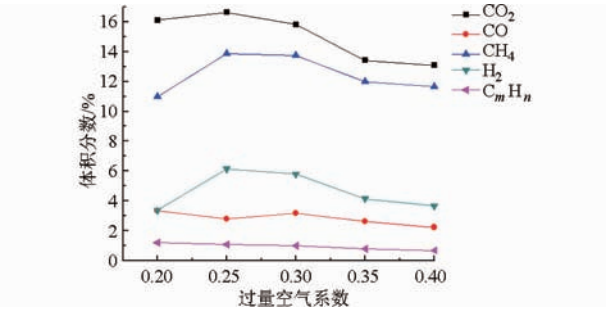


图 11 燃气成分体积分数随过量空气系数的变化

Fig. 11 Variations of gas composition with ER

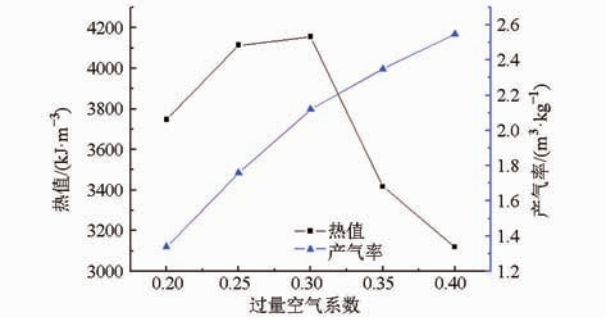


图 12 热值与产气率随过量空气系数的变化

Fig. 12 Variations of gas LHV and gas yield with ER

样是衡量气化效果的重要指标,其数值直接说明了整个气化过程的运行效率以及经济性。从图 13 中可以看出,在过量空气系数较小时,气化效率和碳转化率均随过量空气系数的增大而增大,气化效率和碳转化率在为 0.3 时达到实验的最高值,随后 2 个指标均有下降趋势。分析原因,气化剂使燃气部分燃烧,不可燃组分的增多使燃气热值快速降低;碳转化率的降低则由于回转炉内气体流速增加,携带出炉的碳含量增多,实验结果与文献[15]的报道接近。

## 2.4 典型工况分析

在过量空气系数 0.2 ~ 0.4 变化的变工况实验

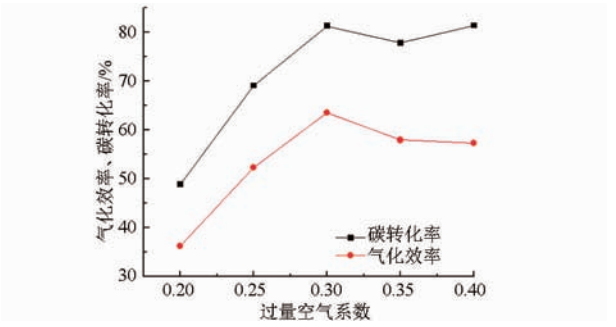


图 13 碳转化率和气化效率随过量空气系数的变化

Fig. 13 Variations of carbon conversion efficiency and gasification efficiency with ER

中选取 0.3 作典型工况分析:工况给料量 2.6 kg/h,回转炉转速维持 3 r/min,监测床料区平均测点温度约为 700℃,床料区温度在回转炉转速较大时相对均匀;回转炉上部气相空间温度约为 570℃,燃料在该处加热、干燥以及热解使该处温度低于床料区。引出回转式气化反应器的产品气进入二燃室燃烧,燃烧室下、中、上部热电偶距离燃烧器底部分别为 300、700、1 000 mm 的位置,温度分别约为 924、1 000、840℃,监测二燃室燃尽排放烟气中 CO 体积分数约为 $1.5\times10^{-4}$ ~ $2.0\times10^{-4}$,$NO_x$ 体积分数约为 $2.0\times10^{-4}$ ~ $4.0\times10^{-4}$。

### 2.4.1 燃气状况分析

收集稳定气化工况的产品气,利用气相色谱分析其组分并与鼓泡流化床和循环流化床生物质气化典型燃气成分对比,如表 1 所示,该回转气化反应器的燃气成分与流化床气化基本类似。从某种程度上,可以将该类气化炉看做一种特殊流化床,只是用机械扰动代替了流化风,由于无需考虑流化风和床料颗粒之间的协调,在调节上具有更大灵活性。

**表 1 回转气化炉典型工况下的产气成分(体积分数)**

**Tab. 1 Gas composition of rotary gasifier under typical operation condition** %

| 炉型 | CO | $CO_2$ | $H_2$ | $CH_4$ | $C_mH_n$ | $N_2$ | $O_2$ |
|---|---|---|---|---|---|---|---|
| 回转气化炉 | 13.75 | 15.82 | 5.51 | 3.17 | 0.99 | 58.77 | 0.93 |
| 鼓泡流化床[22] | 13 ~ 16 | 10 ~ 14 | 4 ~ 8 | 3 ~ 7 | 1.5 ~ 2.9 | 45 ~ 55 | 0.8 ~ 2 |
| 循环流化床[22] | 14 ~ 23 | 7 ~ 15 | 4 ~ 8 | 4 ~ 10 | 1 ~ 2.5 | 45 ~ 60 | 0.8 ~ 2 |

针对该回转气化反应器运行的定量评估参数,其中碳转化率为生物质燃料中的碳转化为气体燃料中碳的份额,计算方法为[20]

$$\eta_c=\frac{M_{CH_xO_y}(C_{CO}+C_{CO_2}+C_{CH_4}+2.5C_{C_mH_n})}{22.4}G_y$$

式中,$C_{CO}$、$C_{CO_2}$、$C_{CH_4}$、$C_{C_mH_n}$ 分别表示相应气体在气化气中的体积分数,$M_{CH_xO_y}$ 是指生物质的特征分子式的分子量,由生物质的元素分析比例化简得到,$G_y$ 表示产气率。本研究所用生物质特征分子式为 $CH_{1.5}O_{0.68}$,特征分子量约为 24.4,计算碳转化率为 81.3%;计算气体产率约为 2.1 $m^3$/kg,同时得到该气化炉冷态气化效率为 64.3%,考虑显焓的气化效率约为 79.3%。

典型实验结果显示,空气作为气化介质产生燃气热值约为 4 156 kJ/$m^3$,相对较低,主要由于产品气采集测量过程中焦油被冷凝除去,所含能量未能计入产品气,以及小型实验设备散热损失较大等原因。

### 2.4.2 能量平衡分析

实验系统的能量平衡特点也是衡量气化燃烧装

置效用的评价方式之一，通过能量平衡计算，可以判断该系统各部分能量流的分布，计算能量转换效率以及各项热损失，为提高反应效率提供数据支撑[23]。

实验系统中的气化过程稳态工况工作时，进入系统的能量等于离开系统的能量总和，具体能量流程如图 14 所示，图中所有能量对应于单位质量的燃料。系统中燃料和气化剂携带能量进入气化炉，包括气化炉散热和残碳热损失，以及焦油带出能和热燃气带出的化学能 $Q_g$、焦油化学能 $Q_{Tar}$和物理显热 $Q_H$。焦油与热燃气携带能量进入二燃室实现向烟气显热的完全转化过程，该过程充分利用了焦油和燃气显热所携带的热量。

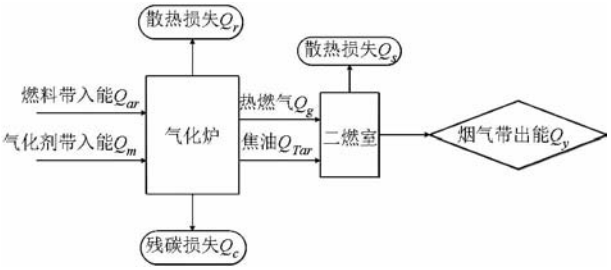


图 14　实验系统的能量平衡体系

Fig. 14　Energy balance system of experiment

由于焦油和热燃气均作为燃料进入二燃室燃烧利用，均为系统的有效利用能量，气化炉作为能量转化的核心部分，其能量平衡方程为

$$Q_{ar} + Q_m = Q_g + Q_H + Q_{Tar} + Q_r + Q_c$$

各部分能量计算方法参照文献[22]，以标准环境为计算背景，结果如表 2 所示。

**表 2　气化系统能量平衡结果**

**Tab. 2　Energy balance results of gasification system**

| | 项目 | 热量/kJ | 比例/% |
|---|---|---|---|
| 输入能 | $Q_{ar}$ | 13 724 | 95. 5 |
| | $Q_m$ | 643 | 4. 5 |
| 有效能 | $Q_g$ | 8 830 | 61. 4 |
| | $Q_H$ | 2 150 | 15. 0 |
| | $Q_{Tar}$ | 1 494 | 10. 4 |
| | 合计 | 12 474 | 86. 8 |
| 能量损失 | $Q_r$ | 1 565 | 10. 4 |
| | $Q_c$ | 329 | 2. 8 |
| | 合计 | 1 894 | 13. 2 |

表 2 中计算结果显示，以气化炉为核心的能量平衡，以气化炉为核心的能量平衡，有效能约占总输入量的 86. 8%，13. 2% 的能量损失中散热损失 $Q_r$为主要能量损失，小型实验台的保温效果不足，有待改进。

### 2. 4. 3　底灰分布分析

反应器中半焦的气固相反应是生物质气化的主要过程，分析气化炉床料中底灰、半焦的粒径形态有助于理解气化反应器的运行特性。

在稳定运行工况结束后，用多孔筛网将底灰与床料分离，由于床料粒径在 3 ~ 5 mm，选用网孔直径在 2. 5、1. 25、0. 5、0. 3 mm 4 种粒径的筛网对底灰进行分离，对应不同粒径的底灰颗粒形态如图 15 所示。其中，左边 4 幅分别对应 4 种筛网分离的底灰，右上角为气化炉内基本维持生物质颗粒原始状态的焦炭图样，右下角为床料与焦炭混合在一起的状态。

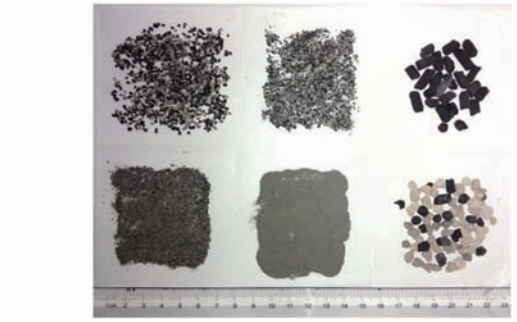

图 15　不同粒径分布的底灰形态图

Fig. 15　Bottom ash morphology of different particle sizes

从图 15 中可以看出，底灰的形态分布显示，机械扰动和床料均温作用下的底灰无明显结渣。右侧的样本分别是焦炭与床料焦炭混合物，其中焦炭颗粒表面灰分很少，且焦炭床料在炉内混合相对均匀。实验结果显示，床料区生物质热解焦炭颗粒与床料具有较好的混合特性。

为了定量分析回转炉内生物质灰的分布，将静止状态下的炉内床料按上下位置等质量均分为 2 份，分别对其中灰进行分离筛分称量，结果如表 3 所示。

**表 3　床料区底灰分布**

**Tab. 3　Bottom ash distribution in bed material area**

g

| 位置 | 粒径分布/mm | | | |
|---|---|---|---|---|
| | 0 ~ 0. 3 | 0. 3 ~ 0. 5 | 0. 5 ~ 1. 2 | 1. 2 ~ 2. 5 |
| 上部 | 90. 0 | 23. 6 | 20. 4 | 18. 0 |
| 下部 | 1 087. 5 | 328. 2 | 152. 6 | 87. 4 |

由表 3 数据可见，床料区的所有灰渣中中小粒径灰占主体，其中粒径在 0. 5 mm 以下的底灰占总质量的 85%。另一方面，根据床料分层取样的结果，底灰分布主要集中在床料区下部，且占床料区底灰总质量的 90% 以上，这对于床料与底灰的分离，以及排渣口的设计具有参考价值。

## 3　结论

(1)以生物质颗粒为原料进行的部分空气气化实现该回转式气化反应器可以很好地控制气化反应区温度，确保气化过程顺利进行，同时产品气可以在

后续燃烧装置中燃烧以完成分级燃烧过程。

(2)实验证实了回转炉转速增加影响回转炉混合扰动特性以及炉内温度分布,进而对生物质气化反应的特征参量具有重要影响。且在一定范围内随转速增大,燃气热值、产气率、气化效率以及碳转化率均有提高,在实验范围内回转炉转速在 3 r/min 时,取得较好的产气结果,随后影响程度减缓。

(3)实验中采用同时调节给料与一次风保证过量空气系数不变的情况下,改变温度,实验结果表明:在实验变量范围内,可燃气组分、热值、气化效率以及碳转化率等指标均随温度升高有增大趋势,其中燃气热值、气化效率受温度影响较大,实验条件下 600 ~650℃温度范围内燃气热值和气化效率等指标有较大提升。

(4)过量空气系数对产气结果的各项指标均有较大影响,实验范围内随过量空气系数增加,除产气率和床料区温度在一定程度增大外,产气中可燃气组分、热值、气化效率以及碳转化率均有先增大后减小的变化趋势,实验中过量空气系数为 0.3 时气化效果最好。

(5)测试过量空气系数选取 0.3 典型工况下测试回转气化炉产气组分,与流化床气化炉气化组分对比可见,该回转式气化炉的气化效果与流化床炉型接近;同时得到该气化炉冷态气化效率 64.3%,考虑显焓的气化效率约为 79.3%、碳转化率约为 81.3%;以气化炉为核心进行能量平衡计算,结果显示有效能约占总输入部分的 86.8%,13.2% 的能量损失中散热损失 $Q_l$ 为主要能量损失,系统保温有待改进。

(6)分离床料区的底灰后发现,床料区滞留的底灰超过 90% 停留在床料区下部,生物质底灰与床料具有较好的回转分离效果,且大部分底灰粒径较小;底灰的形态分布显示,机械扰动和床料均温作用下的底灰无明显结渣。

## 参 考 文 献


1 杨倩,曾令可. 我国回转炉技术现状及特点[J]. 陶瓷,2010(2):44 - 49.
YANG Qian, ZENG Lingke. Status and characteristics of the domestic furnace[J]. Ceramics,2010(2):44 - 49. (in Chinese)

2 池涌,张志宵,阎大海,等. 综合流动和传热的废轮胎回转窑热解模型[J]. 工程热物理学报,2004,25(2):333 - 336.
CHI Yong, ZHANG Zhixiao, YAN Dahai, et al. Movement and heat transfer modeling of tire pyrolysis in a rotary kiln[J]. Journal of Engineering Thermophysics,2004,25(2):333 - 336. (in Chinese)

3 李清水,池涌,李润东,等. 基于 3T 思想的城市垃圾回转炉焚烧系统的设计[J]. 动力工程,2002,22(5):1983 - 1989.
LI Qingshui, CHI Yong, LI Rundong, et al. Municipal solid waste rotary kiln incinerator design with respect to 3T principles[J]. Power Engineering,2002,22(5):1983 - 1989. (in Chinese)

4 马建录,杨传芳. 污泥焚烧回转炉的运行控制[J]. 工业用水与废水,2003,34(1):68 - 70.
MA Jianlu, YANG Chuanfang. Controlling of operation of sludge rotary incinerator[J]. Industrial Water & Wastewater, 2003, 34(1):68 - 70. (in Chinese)

5 文世恩,池涌,张志宵,等. 废轮胎中试回转窑热解炭特性分析[J]. 燃烧科学与技术,2003,9(2):186 - 189.
WEN Shien, CHI Yong, ZHANG Zhixiao, et al. Study on characteristics of pyrolytic char from pyrolysis of scrap tires in a pilot-scale rotary kiln[J]. Journal of Combustion Science and Technology, 2003,9(2):186 - 189. (in Chinese)

6 张志宵. 废轮胎回转窑热解特性及应用研究[D]. 杭州:浙江大学,2004.

7 陈文仲,王春华,田远航,等. 回转窑热工状况影响参数的数值模拟[J]. 化工学报,2011,62(1):47 - 52.
CHEN Wenzhong, WANG Chunhua, TIAN Yuanhang, et al. Numerical simulation on influence factors of thermal working conditions in carbon rotary kilns[J]. Journal of Chemical Industry and Engineering (China),2011,62(1):47 - 52. (in Chinese)

8 杨华,陈全明,薛东卫,等. 一种废弃物回转窑焚烧炉的创新设计[J]. 机械,2004,31(2):48 - 49.
YANG Hua, CHEN Quanming, XUE Dongwei, et al. Innovative design on waste rotary kiln incinerators[J]. Machinery, 2004, 31(2):48 - 49. (in Chinese)

9 ELATTAR H F, STANEV Rayko, SPECHT Eckehard, et al. CFD simulation of confined non-premixed jet flames in rotory kilns for gaseous fuels[J]. Computers Fluids, 2014,102:62 - 73.

10 HERZ F, MITOV I, SPECHT E, et al. Influence of the motion behavior on the contact heat transfer between the covered wall and solid bed in rotary kilns[J]. Experimental Heat Transfer, 2015,28(2): 174 - 188.

11 THAMMABONG Phahath, DEBACQ Marie, VITU Stéphane, et al. Experimental apparatus for studying heat transfer in externally heated rotary kilns[J]. Chemical Engineering Technology, 2011,34(5):707 - 717.

12 王纯良. 循环流化床国内外现状分析[J]. 节能技术,2011,29(2):143 - 144.
WANG Chunliang. Analysis of the development of circulating fluidized bed at home and abroad[J]. Energy Conservation Technology,2011,29(2):143 - 144. (in Chinese)

13 贤建伟,范晓旭,韩中合,等. 床料对生物质流化床气化影响的初步实验研究[J]. 可再生能源,2011,29(1):45 - 48.
XIAN Jianwei, FAN Xiaoxu, HAN Zhonghe, et al. Effects of the bed material on biomass gasification in fluidized bed gasifier [J]. Renewable Energy,2011,29(1):45 - 48. (in Chinese)


(下转第 221 页)

LIU Fei, ZHANG Fan, FANG Hui, et al. Analysis of chorophyll in gannan navel orange with algorithm of GA and SPA based on hyperspectral[J]. Spectroscopy and Spectral Analysis, 2009, 29(11):3079－3093. (in Chinese)

18 章海亮,刘雪梅,何勇. SPA－LS－SVM 检测土壤有机质和速效钾研究[J]. 光谱学与光谱分析,2014,34(5):1348－1351.
ZHANG Hailiang, LIU Xuemei, HE Yong. Measurement of soil organic matter and available K based on SPA－LS－SVM[J]. Spectroscopy and Spectral Analysis, 2014, 34(5):1348－1351. (in Chinese)

19 魏远隆,尹昌海,陈贵平,等. 近红外光谱结合主成分分析鉴别不同产地的南丰蜜桔[J]. 光谱学与光谱分析,2013, 33(11):3024－3027.
WEI Yuanlong, YIN Changhai, CHEN Guiping, et al. Identification of Nanfeng mandarin from different origins by using near infrared spectrosopy coupled with principal components analysis[J]. Spectroscopy and Spectral Analysis, 2013, 33(11):3024－3027. (in Chinese)

20 贾伟宽, 赵德安, 阮承治,等. 苹果夜视图像小波变换与独立成分分析融合降噪方法[J]. 农业机械学报,2015, 46(9):9－17.
JIA Weikuan, ZHAO Dean, RUAN Chengzhi, et al. Combined method for night vision image denoising based on wavelet transform and ICA[J]. Transactions of the Chinese Society for Agricultural Machinery, 2015, 46(9):9－17. (in Chinese)

21 李朝晖,粘永健. 基于独立分量分析的高光谱图像降维与压缩算法[J]. 计算机与数字工程,2014,42(8):1472－1475.
LI Zhaohui, NIAN Yongjian. Dimensionality reduction and compression of hyperspectral imagery based on independent component analysis[J]. Computer and Digital Engineering, 2014, 42(8):1472－1475. (in Chinese)

(上接第 214 页)

14 范晓旭,贤建伟,初雷哲,等. 生物质鼓泡流化床和循环流化床对比试验[J]. 农业机械学报,2011,42(4):96－99.
FAN Xiaoxu, XIAN Jianwei, CHU Leizhe, et al. Comparison of bubbling fluidized bed and circulating fluidized bed in gasification of biomass[J]. Transactions of the Chinese Society for Agricultural Machinery, 2011,42(4):96－99. (in Chinese)

15 谢军,吴创之,陈平,等. 中型流化床中的生物质气化实验研究[J]. 太阳能学报,2007,28(1):86－90.
XIE Jun, WU Chuangzhi, CHEN Ping, et al. An experimental study on biomass gasification in a medium fluidized bed gasifier [J]. Acta Energiae Solaris Sinica, 2007,28(1):86－90. (in Chinese)

16 盖超,董玉平. 下吸式固定床生物质气化温度场和组分场分布特性[J]. 农业机械学报,2012,43(5):91－96.
GAI Chao, DONG Yuping. Temperature distribution and gas composition of biomass gasification in downdraft fixed bed gasifier [J]. Transactions of the Chinese Society for Agricultural Machinery, 2012, 43(5):91－96. (in Chinese)

17 姚宗路,孟海波,田宜水,等. 抗结渣生物质固体颗粒燃料燃烧器研究[J]. 农业机械学报,2010,41(11):89－93.
YAO Zonglu, MENG Haibo, TIAN Yishui, et al. Design and experiment on anti-slagging biomass pellet fuel burner[J]. Transactions of the Chinese Society for Agricultural Machinery,2010,41(11):89－93. (in Chinese)

18 谭力. 生物质燃烧过程中碱金属迁移及结渣特性的研究[D]. 北京:华北电力大学,2014.

19 黄芳. 秸秆燃烧过程中受热面沉积腐蚀问题研究[D]. 杭州:浙江大学,2012.

20 臧云浩,刘运权,王夺,等. 两级下吸式生物质气化炉气化性能的研究[J]. 可再生能源,2014,32(6):836－841.
ZANG Yunhao, LIU Yunquan, WANG Duo, et al. Study on gasification performance of a two-stage downdraft gasifier[J]. Renewable Energy Resources,2014,32(6):836－841. (in Chinese)

21 潘贤齐,苏德仁,周肇秋,等. 生物质流化床气化中试试验研究[J]. 农业机械学报,2014,45(10):175－179.
PAN Xianqi, SU Deren, ZHOU Zhaoqiu, et al. Experimental investigation of biomass gasification in a pilot-scale fluidized bed gasifier [J]. Transactions of the Chinese Society for Agricultural Machinery,2014,45(10):175－179. (in Chinese)

22 孙立,张晓东. 生物质热解气化原理与技术[M]. 北京:化学工业出版社,2012.

23 初雷哲,范晓旭,肖琦,等. 双循环流化床生物质解耦气化实验[J]. 农业机械学报,2010,41(增刊):117－120.
CHU Leizhe, FAN Xiaoxu, XIAO Qi, et al. Dual fluidized bed biomass decoupled gasification experiments [J]. Transactions of the Chinese Society for Agricultural Machinery,2010,41(Supp.):117－120. (in Chinese)

24 赖喜锐,周肇秋,刘华财,等. 生物质灰烧结熔融规律实验研究[J]. 农业机械学报,2016,47(3):158－166.
LAI Xirui, ZHOU Zhaoqiu, LIU Huacai, et al. Experiment study of biomass ash sintering and melting[J]. Transactions of the Chinese Society for Agricultural Machinery, 2016,47(3):158－166. (in Chinese)

25 姚宗路,吴同杰,赵立欣,等. 生物质固定燃烧源烟气稀释采样装置设计与试验[J]. 农业机械学报,2016,47(3):174－178.
YAO Zonglu, WU Tongjie, ZHAO Lixin, et al. Design and experiment of flue gas dilution sampler for biomass fixed combustion source[J]. Transactions of the Chinese Society for Agricultural Machinery, 2016,47(3):174－178. (in Chinese)

26 姚锡文,许开立,徐晓虎. 灰化温度对生物质灰特性与沾污结渣的影响[J]. 农业机械学报,2016,47(1):182－189.
YAO Xiwen, XU Kaili, XU Xiaohu. Influence of ashing temperature on slagging and fouling characteristics of biomass ash[J]. Transactions of the Chinese Society for Agricultural Machinery, 2016,47(1):182－189. (in Chinese)